A Quasi-Geostrophic Numerical Model Incorporating Effects of Release of Latent Heat[1]

MAURICE B. DANARD
Meteorological Service of Canada, Toronto

(Manuscript received 4 June 1965, in revised form 8 October 1965)

ABSTRACT

A quasi-geostrophic numerical model for predicting precipitation amounts and the heights of the 1000-, 850-, 700-, 500-, and 300-mb surfaces is described. The basic equations are the vorticity and omega equations. Influences of released latent heat are incorporated in the static stability in the latter equation. Frictional and orographic effects are included in the lower boundary condition for the vertical velocity.

Numerical integrations are carried out for 36 hours in a case of intense cyclogenesis over central United States. "Moist" and "dry" predictions are made, the latter by artificially excluding effects of release of latent heat. In the "dry" prognosis, the sea-level low is moved northeastward but not intensified. By contrast, in the "moist" prediction it is rapidly deepened. Forecast precipitation amounts agree roughly in magnitude with observations. However, the occurrence of heavy convective precipitation along the cold front is not satisfactorily predicted.

1. Introduction

Numerical predictions of precipitation amounts were first carried out by Smagorinsky and Collins (1955). In a subsequent paper, Smagorinsky (1956) pointed out the necessity of including effects of release of latent heat. If these influences were not considered, the computed vertical velocities were underestimated in regions of condensation by as much as an order of magnitude. The amplifying effect of release of latent heat on upward motions has also been demonstrated by Aubert (1957), Smebye (1958), Pedersen (1963), and Danard (1964).

This enhancement of the ascending motion leads to increases in low-level convergence and high-level divergence. As a result, the sea-level low tends to intensify and move with the center of heaviest precipitation. In the upper troposphere, the precipitation maximum may often be located under the region of strong anticyclonic shear on the warm air side of the jet. The increase in divergence at high levels then leads to an intensification of the anticyclonic relative vorticity there. However, the middle troposphere is very nearly nondivergent no matter whether release of latent heat is considered or not. Consequently, vorticity changes at these levels would normally be little affected by the occurrence of condensation. A similar vertical variation (i.e., marked influences at low and high levels but little effect in the middle troposphere) was noted by Danard (1964) in examining the role of release of latent heat in changes of kinetic energy of the atmosphere.

[1] A summary of this paper was presented at the Annual Meeting of the Canadian Branch of the Royal Meteorological Society held in Vancouver, B. C., on 8–9 June 1965.

This paper describes an attempt to incorporate the influences of released latent heat into a numerical prediction model. Probably the most important problems here are the computation of the vertical velocity and the prediction of the moisture field (Sections 2 and 3). The author is aware that more elaborate techniques than employed here could have been used. For example, the balance equation could replace (2). Further, the lower boundary condition for ω $(=dp/dt)$ could be applied at the actual terrain pressure rather than at 1000 mb. Nevertheless, it is believed that the methods described here suffice to demonstrate the effects of release of latent heat in the numerical prediction of cyclone development. Refinements such as those noted above would probably be necessary, however, in an operational scheme.

2. General description of the model

This paper describes a numerical method for predicting precipitation amounts and the heights of the 300-, 500-, 700-, and 850-mb surfaces. In addition, the 1000-mb height is obtained from a simple relation with the 850- and 700-mb levels.

The basic procedure may be described with the aid of Fig. 1. First, ω is set equal to zero at 200 mb and computed at 400, 600, 775, and 1000 mb using the techniques described in Section 3. Effects of release of latent heat are of prime importance in determining the vertical velocity. The vorticity equation is then applied at 300, 500, 700, and 850 mb to obtain the predicted height fields. These height fields, together with the predicted moisture field, are used to compute the new

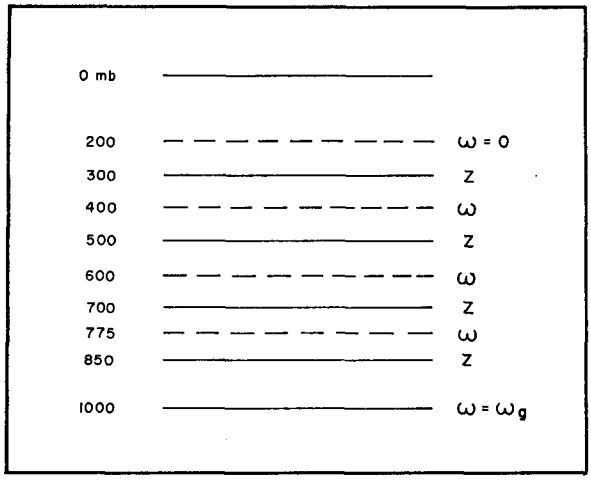

FIG. 1. Model of the atmosphere used for numerical integration.

ω and the procedure is repeated. The form of the vorticity equation used is

$$\frac{\partial \zeta_g}{\partial t} = -\mathbf{V}_g \cdot \nabla(\zeta_g + f) + f_0 \frac{\partial \omega}{\partial p} + K\nabla^2 \zeta_g, \tag{1}$$

where non-divergence of the advecting wind is ensured by defining

$$\mathbf{V}_g = \frac{g}{f_c}\mathbf{k} \times \nabla Z. \tag{2}$$

In (1), ζ_g is the geostrophic vorticity, f_0 is the standard value of the coriolis parameter, and K is the coefficient of horizontal eddy diffusivity.

The coefficient K was computed by Grimminger (1941) by observing the diffusion of specific humidity on upper-level charts. He found values ranging from 3×10^8 to 3.9×10^{10} cm^2 sec^{-1}, the mean being 5.5×10^9 cm^2 sec^{-1}. The figure chosen for use in (1) was 4×10^9 cm^2 sec^{-1}. It will be noted that the inclusion of an eddy diffusion term also serves to suppress spurious small-scale perturbations arising from computational procedures. It may be readily verified that if one uses the simple 5-point formula for computing the Laplacian and the grid size customarily employed in North America (381 km at 60N), then setting $K=4\times10^9$ cm^2 sec^{-1} is approximately equivalent to applying the smoothing operator (11) every 12 hours. In integrating (1) the diffusion term was evaluated from data of the previous, rather than the current, time step. This was necessary to avoid computational instability [see, e.g., Richtmyer (1957), pp. 93–94].

3. Computing the vertical velocity

Inclusion of effects of release of latent heat. The quasi-geostrophic ω-equation for non-adiabatic motion may be written (Petterssen *et al.*, 1962) as

$$\sigma_0\nabla^2\omega + f_0^2\frac{\partial^2\omega}{\partial p^2} = -g\nabla^2\mathbf{V}_g\cdot\nabla\frac{\partial Z}{\partial p} + f_0\frac{\partial}{\partial p}\mathbf{V}_g\cdot\nabla(\zeta_g+f) - \frac{R}{C_p p}\nabla^2 H, \tag{3}$$

where $\sigma_0(p)$ is a standard value over an isobaric surface of the static stability parameter $\sigma = -\alpha\partial\ln\theta/\partial p$, and H is the input of heat per unit mass. Assuming the main contribution to H is from released latent heat, then

$$H = -L_v\frac{dr_s}{dp}\omega\delta_s, \tag{4}$$

where dr_s/dp is the rate of change, following the motion, of the saturation mixing ratio r_s with p, and $\delta_s(x,y,p)$ is unity or zero according as the point in question is saturated or not. Eq. (3) may then be written

$$\nabla^2\hat{\sigma}\omega + f_0^2\frac{\partial^2\omega}{\partial p^2} = -g\nabla^2\mathbf{V}_g\cdot\nabla\frac{\partial Z}{\partial p} + f_0\frac{\partial}{\partial p}\mathbf{V}_g\cdot\nabla(\zeta_g+f), \tag{5}$$

where

$$\hat{\sigma} = \sigma_0 - \frac{RL_v}{C_p p}\frac{dr_s}{dp}\delta_s. \tag{6}$$

Thus, if $Z(x,y,p)$ and $\delta_s(x,y,p)$ are known and appropriate boundary conditions are applied, one can solve (5) for ω. Note that the inclusion of released latent heat is formally identical to permitting horizontal variations in the static stability. Since $\hat{\sigma}$ is a minimum in saturated regions, this will result in an increase in the magnitudes of the computed vertical motions.

It is evident that $\hat{\sigma}$ and ω will, in general, be positively correlated. By integrating the thermodynamic equation over a closed isobaric surface, it is readily seen that this will tend to increase the average temperature. Thus, there is an upper limit to the time interval during which it is permissible to neglect other heat sources and sinks.

The values of σ_0 at 400, 600, and 775 mb are set equal to 3.73×10^{-4}, 2.26×10^{-4}, and 2.27×10^{-4} gm^{-2} cm^4 sec^2, respectively. These are obtained by interpolation from the mean January values over the United States as determined by Gates (1961).

Condensation is assumed to occur in the region between 1000 and 300 mb. For simplicity, vertical variations in $\delta_s(x,y,p)$ in (6) are generally ignored. This factor is replaced by $\Delta_s(x,y)$ defined by

$$\Delta_s(x,y) = 1 - \frac{T-T_d}{7.5} \quad \text{for } (T-T_d)<7.5\text{C}$$
$$\Delta_s(x,y) = 0 \quad \text{otherwise.} \tag{7}$$

The quantity $\Delta_s(x,y)$ may be interpreted as the fraction of the atmospheric column which is saturated. The values of $(T-T_d)$ should be representative of conditions in the troposphere. Here they are approximated by the average of the values at 850, 700, and 500 mb. In regions where the terrain pressure p_t is less than 1000 mb, the following modifications are made:

$$1000>p_t\geqslant 850 \text{ mb}: \quad (\delta_s)_{775}=\Delta_s(p_t-850 \text{ mb})/(150 \text{ mb})$$

$$850>p_t\geqslant 650 \text{ mb}: \quad (\delta_s)_{775}=0$$

$$(\delta_s)_{600}=\Delta_s(p_t-650 \text{ mb})/(200 \text{ mb}).$$

The above procedure is an approximate way of accounting for the effect of variable terrain pressure on the thickness of the precipitating column.

Frictional and orographic effects are used to compute $\omega=\omega_g$ at 1000 mb; discussion of this procedure will be deferred to the next subsection. Using this boundary condition, setting ω equal to zero at 200 mb, and replacing the derivatives by finite differences, (5) can be solved for ω at 400, 600, and 775 mb. Precipitation is computed by assuming the 1000–850 mb layer ascends with velocity ω_g, and the layers 850–700, 700–500, and 500–300 mb with velocities at 775, 600, and 400 mb, respectively. To facilitate this computation, Table 1 gives the rate of condensation per unit vertical velocity at the midpoints of the layers. The values were obtained from those provided by Fulks (1935).

The term dr_s/dp in (6) is obtained by multiplying the values in Table 1 by 2.72×10^{-7} cgs units. Negative values of $\hat{\sigma}$ (i.e., in cases of large dr_s/dp) are set equal to zero to avoid hyperbolicity in (5). It may readily be shown that with the given values of σ_0, $\hat{\sigma}$ would otherwise be negative in saturated air for temperatures exceeding the following: 400 mb,–17C; 600 mb,–5C; 775 mb, 15C.

The temperatures for use in Table 1 are obtained from the forecast thickness fields. It may be remarked that if a stream function is used, the temperature field must be predicted separately.

Lower boundary condition. Neglecting the pressure tendency, the vertical velocity at the top of the planetary boundary layer may be expressed as

$$\omega_g=\omega_t+\omega_f, \tag{8}$$

where ω_t and ω_f are the vertical velocities induced by orographic and frictional influences, respectively.

In regions where ω_t is large, the terrain height is normally of the order of a kilometer or more. Consequently, ω_t is approximated by

$$\omega_t=(\mathbf{V}_g)_{850}\cdot\nabla p_t, \tag{9}$$

where p_t is the standard atmosphere pressure at the elevation of the smoothed terrain provided by Berkofsky and Bertoni (1955) and $(\mathbf{V}_g)_{850}$ is the geostrophic wind at 850 mb.

TABLE 1. Rate of precipitation (mm hr^{-1}) from a 100-mb saturated layer ascending pseudo-adiabatically at a velocity of 1×10^{-3} mb sec^{-1}.

Temperature (deg C)	Pressure (mb) 925	775	600	400
−50	0.001	0.001	0.002	0.005
−45	0.002	0.002	0.004	0.008
−40	0.003	0.004	0.008	0.015
−35	0.005	0.007	0.011	0.024
−30	0.008	0.010	0.015	0.035
−25	0.011	0.014	0.023	0.049
−20	0.015	0.021	0.032	0.065
−15	0.021	0.029	0.044	0.086
−10	0.028	0.037	0.058	0.108
−5	0.035	0.047	0.070	0.131
0	0.044	0.058	0.085	0.152
5	0.053	0.068	0.098	0.170
10	0.061	0.079	0.111	
15	0.070	0.089	0.123	
20	0.077	0.096		
25	0.085	0.104		
30	0.090	0.110		
35	0.095	0.116		

The frictionally induced vertical velocity is computed in the manner suggested by Cressman (1960);

$$\omega_f=-\frac{g}{\alpha f}\mathbf{k}\cdot\nabla\times C_d V_g\mathbf{V}_g. \tag{10}$$

Here, $\mathbf{V}_g$ is a representative geostrophic wind in the planetary boundary layer and C_d is the drag coefficient. From the Ekman theory it may be shown that the maximum mass transport occurs at a height $h/4$, where h is the depth of the planetary boundary layer. Since $h\sim1$ km, it would normally be preferable to use $(\mathbf{V}_g)_{1000}$ rather than $(\mathbf{V}_g)_{850}$. However, the 1000-mb heights are not directly known and although they may be computed from a simple relation with the 850-and 700-mb levels (see Section 5), the values obtained are only approximate. That is, $(\mathbf{V}_g)_{850}$ is probably a more accurate measure to use in (10) than is the derived $(\mathbf{V}_g)_{1000}$. Accordingly, the former is used here.

The inclusion of friction contributes, in general, to the dissipation of sea-level systems. Further, by expanding the right side of (10), it may be seen that the effects of friction tend to maintain the precipitation center over the region of maximum cyclonic vorticity.

4. Prognostic equation for the dew-point depression

Since the dew-point depression as determined from radiosonde observations reflects small-scale vertical motions as well as errors in measurement, it proved necessary to smooth the initial field using the following operator:

$$\psi_{x,y}{}^*=(4\psi_{x,y}+\psi_{x+d,y}+\psi_{x,y+d}+\psi_{x-d,y}+\psi_{x,y-d})/8. \tag{11}$$

Here ψ is the initial value of a quantity, ψ^* is the smoothed value, and d is the distance between adjacent grid points.

The dew-point depression is predicted, assuming $\partial(T-T_d)/\partial p=0$, from the alternative relations

$$\frac{\partial}{\partial t}(T-T_d)=-\mathbf{V}_g\cdot\nabla(T-T_d)+K\nabla^2(T-T_d) \quad (12a)$$

if $T=T_d$ and $\omega<0$; otherwise

$$\frac{\partial}{\partial t}(T-T_d)=-\mathbf{V}_g\cdot\nabla(T-T_d)+\omega\left\{\frac{d}{dp}(T-T_d)\right\}_\theta +K\nabla^2(T-T_d). \quad (12b)$$

Here the subscript θ denotes a dry-adiabatic process. In (12), $\mathbf{V}_g$ is replaced by $(\mathbf{V}_g)_{700}$ and ω by $(\omega_{775}+\omega_{600})/2$. Since the scale of condensation regions is frequently small compared to that of mid-tropospheric wave patterns, computational difficulties necessitated using a value of K in (12) of 2×10^{10} cm^2 sec^{-1}, five times as large as that employed in (1). However, the value of 2×10^{10} cm^2 sec^{-1} is still within the range reported by Grimminger (1941). As in the case of (1), considerations of computational instability necessitated evaluating the diffusion term in (12) from data for the previous, rather than the current, time step.

From the first law of thermodynamics and the Clausius-Clapeyron equation, it may be shown that

$$\left\{\frac{d}{dp}(T-T_d)\right\}_\theta=\frac{\alpha}{C_p}-\frac{RT_d^2}{0.622L_vp}. \quad (13)$$

For $T\sim T_d=0$C and $p=700$ mb, one obtains

$$\left\{\frac{d}{dp}(T-T_d)\right\}_\theta=9.14\times10^{-2}\text{ deg mb}^{-1}. \quad (13a)$$

The above value has been used in the test integration described in Section 6.

5. Computing the 1000-mb height

Since Z_{1000} is not assumed to be known, it may be computed, with heights expressed in meters, from the hydrostatic relation

$$Z_{1000}=1.8368Z_{850}-0.8368Z_{700}-4.76\Delta T. \quad (14)$$

Here ΔT is the difference, in deg C, between the mean virtual temperatures in the layers 1000–850 and 850–700 mb. This quantity is not known, of course, and some arbitrary value must be assigned to it. For a standard atmosphere sounding, $\Delta T\cong9$C. In the test integration described in Section 6, the value of $\Delta T=5$C was used.

Apart from the assumption that ΔT is constant, (14) is also sensitive to errors in the height fields. For example, suppose there is no error arising from the last term in (14). Let E_{850} and E_{700} denote the standard errors in Z_{850} and Z_{700}, respectively. If errors at 850 and 700 mb are uncorrelated, then the standard error in the computed 1000-mb height is

$$E_{1000}=[(1.8368E_{850})^2+(0.8368E_{700})^2]^{\frac{1}{2}}. \quad (15)$$

This susceptibility to error was the chief reason it was decided in Section 3 to use the 850-, rather than the derived 1000-mb field, in computing the effect of surface drag. Nevertheless, the importance of a prognostic 1000-mb chart probably justifies the use of even a simple relation such as (14) in producing the predicted fields.

6. A sample numerical integration

Numerical integrations were made for 36 hours using conditions at 0000 GMT 21 January 1959 as initial data. The lateral boundaries, on which ω and $\partial Z/\partial t$ were kept equal to zero, were located approximately 1300 km out from the borders of the area shown in Figs. 2–7. Intense cyclogenesis occurred over central United

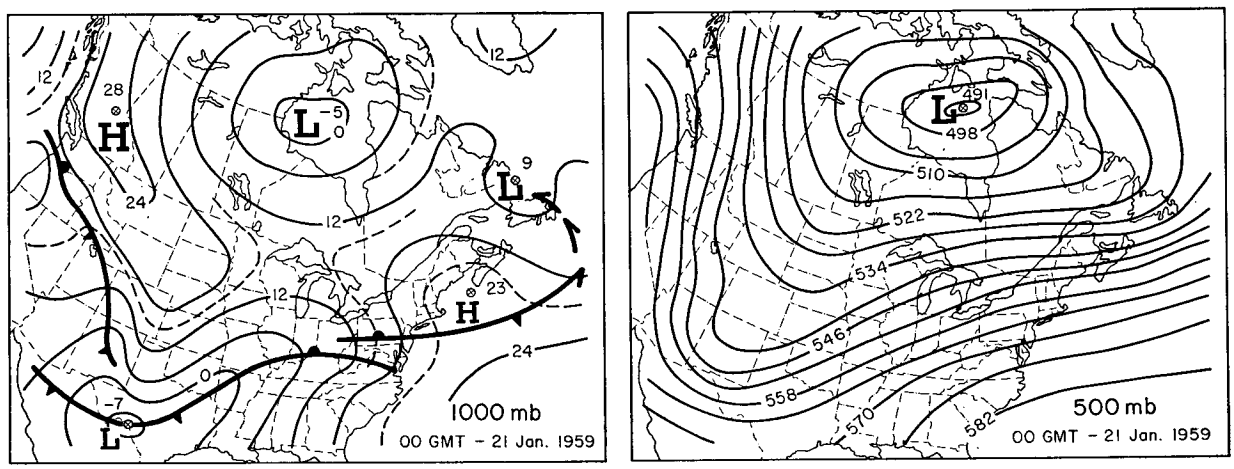

FIG. 2. Initial conditions at 1000 and 500 mb. Units: 10 m.

States during the period. The 1000- and 500-mb charts at the initial time are shown in Fig. 2.

Two predictions were made. In one of these, labelled "moist" in the figures, the actual initial values of $(T-T_d)$ were used. In the other, termed "dry," the initial values of $(T-T_d)$ were assigned fictitiously large magnitudes to ensure that $\Delta_s(x,y)$ in (7) remained everywhere zero during the computations. This excluded effects of release of latent heat.

Heights of isobaric surfaces. In Fig. 3, the "moist" and "dry" predictions at 1000 mb may be compared. The most striking difference is in the treatment of the major cyclone. In the "dry" computations, the low was simply moved northeastward with little change in central height. By contrast, in the "moist" prediction, the low was rapidly deepened. In fact, the forecast intensification somewhat exceeded that which actually occurred. On the other hand, there was little difference between the two predictions of the high in western United States. The erroneous forecast of the low in northwestern United States by both the "dry" and "moist" schemes may be due to shortcomings in the method of considering orographic effects.

TABLE 2. Algebraic mean values (B) and standard deviations (S) of actual height changes (subscript z) and of errors in "moist" and "dry" predictions (subscripts m and d respectively). Values of B and S are in meters.

Level (mb)	Time (hr)	B_z	S_z	B_m	S_m	B_d	S_d
1000	12	19	57	−41	39	−37	38
	24	9	92	−51	58	−37	55
	36	5	125	−68	84	−48	80
850	12	11	40	−14	27	−12	27
	24	7	73	−11	43	−3	47
	36	−9	106	5	72	16	78
700	12	9	38	7	28	7	27
	24	8	69	33	46	34	46
	36	−3	104	69	75	69	80
500	12	10	54	25	35	24	34
	24	21	103	59	66	52	61
	36	11	153	113	111	97	103
300	12	25	81	28	52	25	55
	24	55	144	62	67	50	67
	36	40	213	147	127	122	116

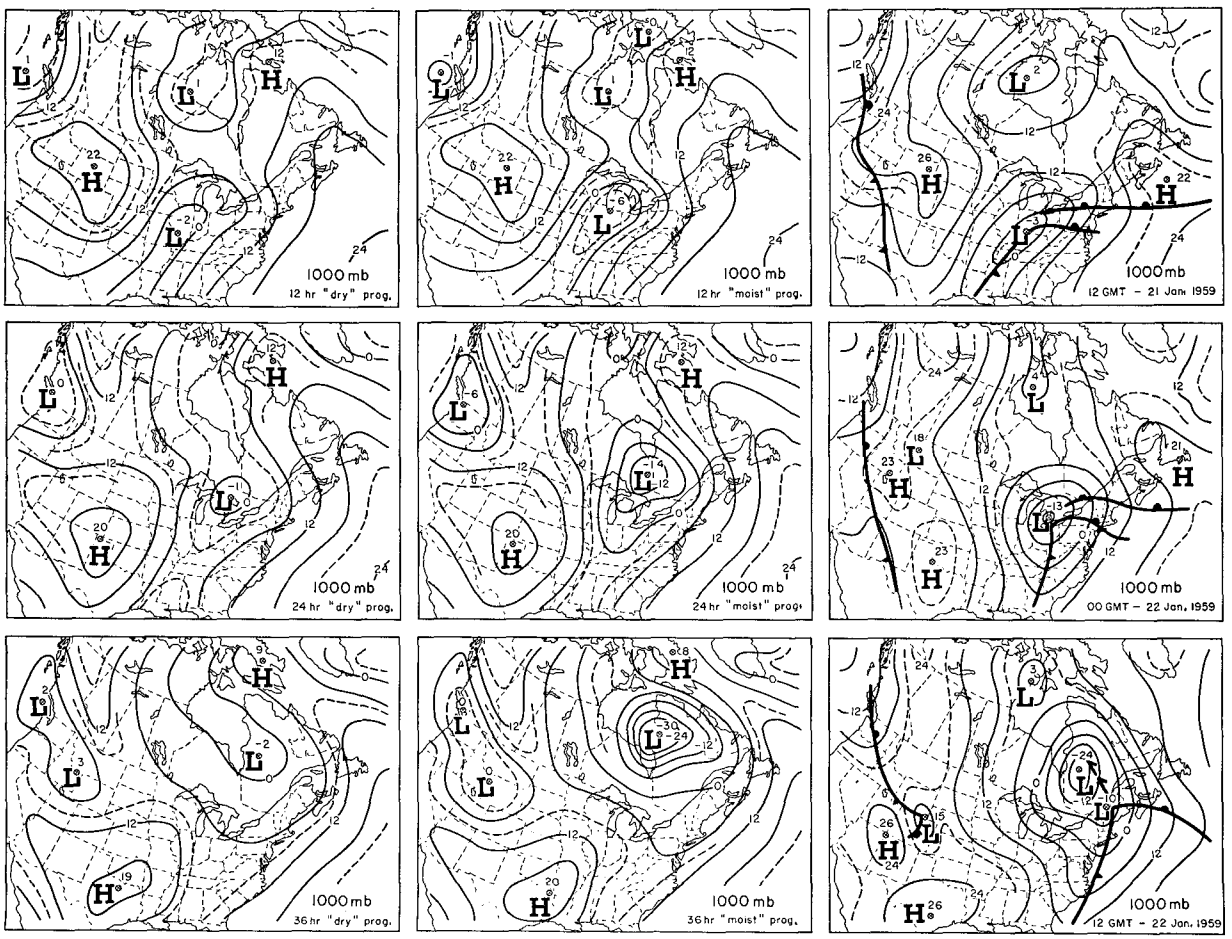

FIG. 3. Comparison of "dry" and "moist" 1000-mb prognoses. Right column: verifying charts. Units: 10 m.

The 500-mb predictions are presented in Fig. 4. As had been anticipated in Section 1, the "moist" and "dry" prognoses are very similar. Both forecasts give too high heights over central Canada. One difference when effects of released latent heat are included appears to be an accentuation of the ridges immediately downstream from the predicted precipitation centers.

Further information on the vertical and temporal variations of the influences of release of latent heat may be gained from a study of Table 2. The values here

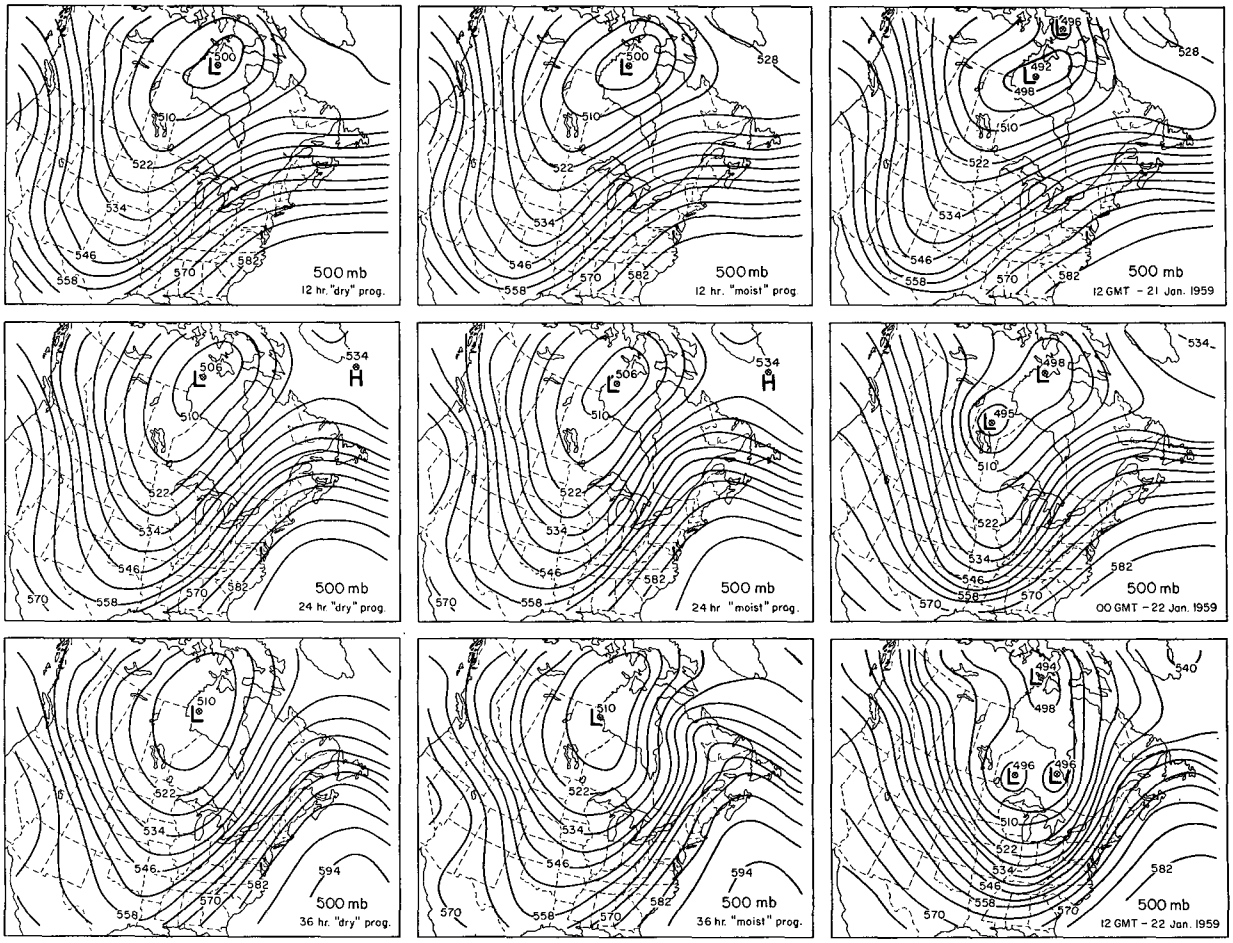

FIG 4. Comparison of "dry" and "moist" 500-mb prognoses. Right column: verifying charts. Units: 10 m.

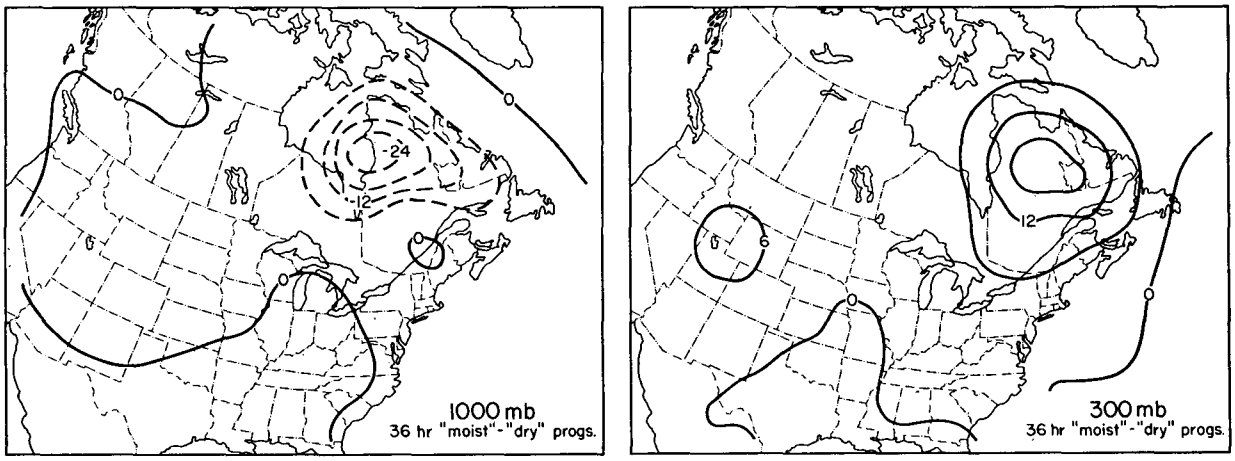

FIG. 5. Height differences between the 36-hr "moist" and "dry" prognoses. Units: 10 m.

were obtained from predicted and actual heights at 192 grid points covering the area shown in Figs. 2–7.

Examining the values of B_m and B_d, it will be noted that both the "moist" and "dry" predictions tend to forecast too low heights in the lower troposphere and too high in the upper troposphere. Further, this bias grows in magnitude with time and is somewhat larger in the "moist" predictions than in the "dry". This is similar to the findings of Aubert (1957) who noted that released latent heat tended to lower heights in the lower troposphere and raise them at higher levels. This effect is clearly demonstrated in Fig. 5. It will also be noted from Table 2 that there is little difference between the "moist" and "dry" predictions at 700 and 500 mb.

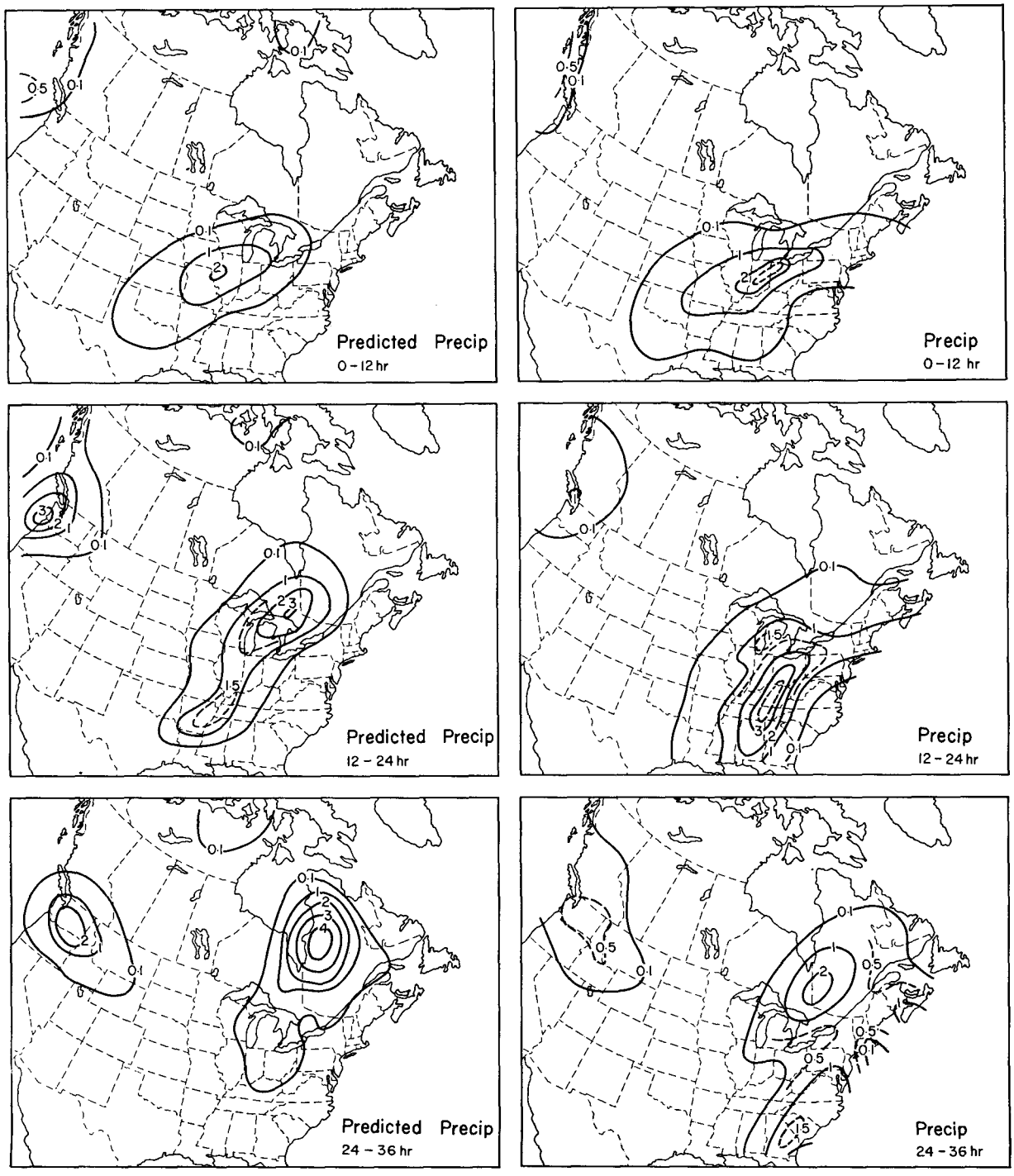

FIG. 6. Predicted and observed precipitation amounts during 36-hr period subsequent to 0000 GMT 21 January 1959. Units: cm.

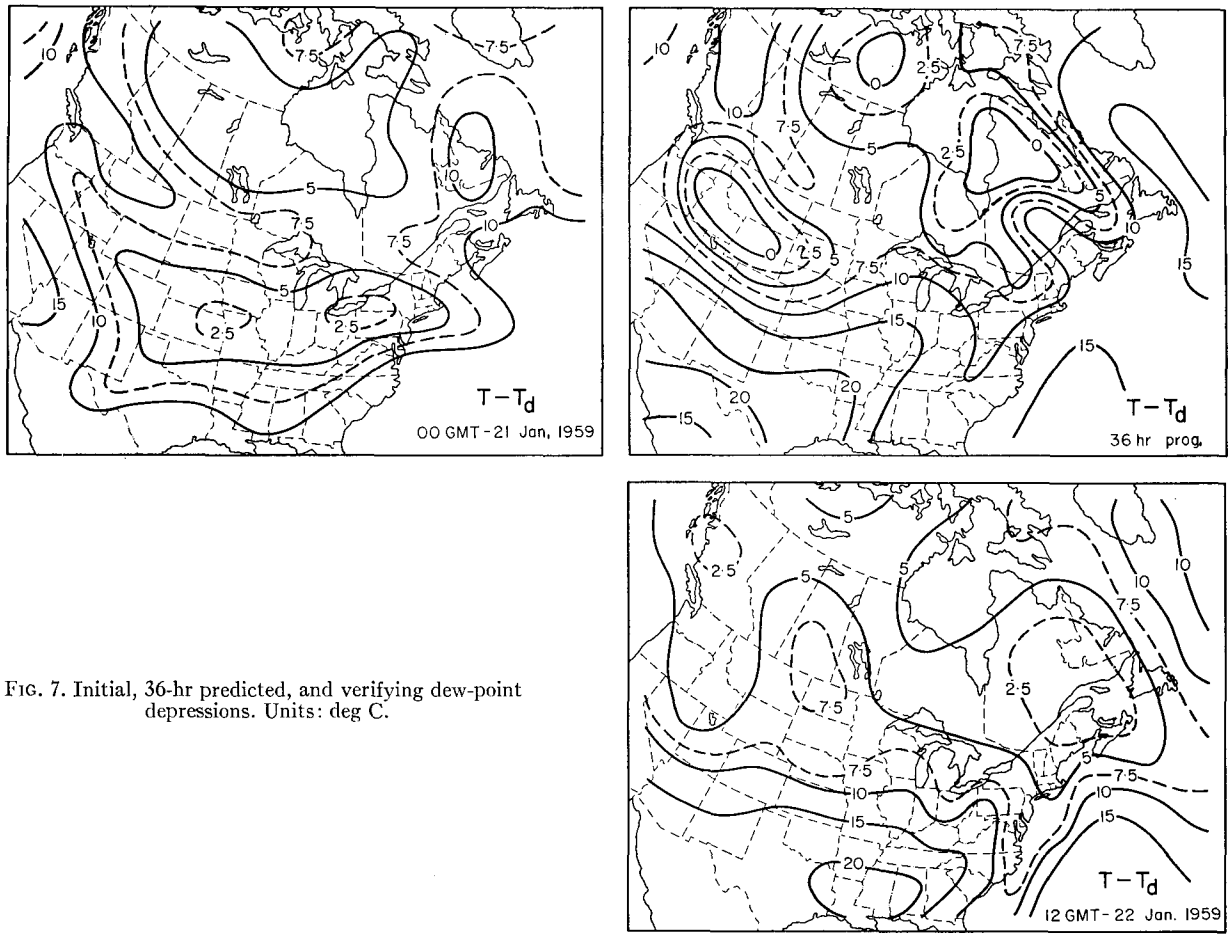

FIG. 7. Initial, 36-hr predicted, and verifying dew-point depressions. Units: deg C.

As has been discussed earlier, this result is not unexpected.

Little systematic difference is evident in Table 2 between the values of S_m and S_d. This may seem surprising in the lower troposphere in view of the apparent better prediction of the cyclone development by the "moist" scheme in Fig. 3 as compared to the "dry." However, most of the contribution to S_m is probably from errors in the forecast location of the major low center. Further, the standard deviation of the height error is a measure of the accuracy of the forecast at a fixed point and may not be the best estimate of the ability to predict the occurrence or non-occurrence of an event such as cyclogenesis.

Precipitation. Predicted and actual precipitation amounts are shown in Fig. 6. In the major precipitation system, much of the error may be attributed to the occurrence of heavy thundershowers along the cold front. Convective precipitation was especially heavy during the daytime period 12–24 hr after the initial time. This type of rainfall cannot, of course, be adequately predicted by a quasi-geostrophic model. For that matter, accounting satisfactorily for showery precipitation is probably one of the most difficult problems in any prediction scheme. As for the precipitation area which crossed the west coast, its shape and the location of its center have been adequately forecast but maximum amounts have been overestimated by a factor of about two. This overestimate may be due to shortcomings in the method used to incorporate orographic influences. It is probably associated with the above-noted excessive deepening of the low in this area by both the "dry" and "moist" predictions.

Dew-point depression. The actual values of $(T-T_d)$ at the initial time and 36 hrs later, smoothed in accordance with (11), and the 36-hr predicted dew-point depressions are shown in Fig. 7. The forecast pattern is consistent with the "moist" 36-hr 1000-mb prognosis given in Fig. 3. However, errors in the latter, such as the incorrect locations of the major low center, the cold frontal trough, and the low over northwestern United States, are reflected in the predicted dew-point depression field. On the other hand, the center of maximum $(T-T_d)$ over Louisiana is fairly accurately predicted. The magnitudes of the forecast gradients are somewhat larger than observed, suggesting that the

use of a larger value of K in (12) might have been preferable.

7. Summary and conclusions

In this paper a procedure to incorporate effects of release of latent heat into a quasi-geostrophic, multilevel numerical prediction model is presented. Precipitation amounts and the heights of the 1000-, 850-, 700-, 500-, and 300-mb surfaces are predicted. The basic equations are the vorticity and omega equations. Influences of released latent heat are included in the static stability in the latter equation. Frictional and orographic effects are incorporated in the lower boundary condition for the vertical velocity. The mean of the dew-point depressions at 850, 700, and 500 mb serves as the moisture parameter.

Numerical integrations are carried out for 36 hours in a case of intense cyclogenesis over central United States. For comparison, "moist" and "dry" predictions are made, the former with the actual initial dew-point depressions and the latter using spuriously large values to exclude effects of release of latent heat. In the "dry" prognosis, the sea-level low is simply moved northeastward but not intensified. On the other hand, in the "moist" prediction, the low is rapidly deepened. Both forecast schemes tend to predict too low heights in the lower troposphere and too high at upper levels. This bias is somewhat larger in the "moist" prediction than in the "dry." Forecast and actual precipitation amounts agree roughly in magnitude. However, the occurrence of heavy convective precipitation along the cold front is not satisfactorily predicted. The forecast dew-point depression field is fairly realistic although spatial variations are somewhat larger than observed.

To sum up, the results suggest that the broad features of the troposphere during cyclogenesis may be predicted by the model described here. It would be wrong, however, to claim unqualified success. In future case studies, efforts should be concentrated on eliminating the shortcomings noted above.

Acknowledgments. The author wishes to express his gratitude to Mr. J. M. Leaver, Officer-in-Charge, Central Analysis Office, Montreal, who made available the synoptic charts and other data for the case studied. Thanks are also due Dr. W. L. Godson and Messrs. D. Davies, T. J. G. Henry, M. Kwizak, and J. Simla for helpful discussions.

REFERENCES

Aubert, E. F., 1957: On the release of latent heat as a factor in large scale atmospheric motions. *J. Meteor.*, **14**, 527–542.

Berkofsky, L., and E. A. Bertoni, 1955: Mean topographical charts of the entire earth. *Bull. Amer. Meteor., Soc.*, **36**, 350–354.

Cressman, G. P., 1960: Improved terrain effects in barotropic forecasts. *Mon. Wea. Rev.*, **88**, 327–342.

Danard, M. B., 1964: On the influence of released latent heat on cyclone development. *J. Appl. Meteor.*, **3**, 27–37.

Fulks, J. R., 1935: Rate of precipitation from adiabatically ascending air. *Mon. Wea. Rev.*, **63**, 291–294 (see also *Smithsonian Meteor. Tables*, 1958, Washington, D. C., Smithsonian Inst., 325–326).

Gates, W. L., 1961: Static stability measures in the atmosphere. *J. Meteor.*, **18**, 526–533.

Grimminger, G., 1941: The intensity of lateral mixing in the atmosphere as determined from isentropic charts. *Bull. Amer. Meteor. Soc.*, **22**, 227–233.

Pedersen, K., 1963: On quantitative precipitation forecasting with a quasi-geostrophic model. *Geofys. Publ.*, **25**, No. 1, 25 pp.

Petterssen, S., D. L. Bradbury and K. Pedersen, 1962: The Norwegian cyclone models in relation to heat and cold sources. *Geofys. Publ.*, **24**, 243–280.

Richtmyer, R. D., 1957: *Difference Methods for Initial-value Problems*. New York, Interscience, 238 pp.

Smagorinsky, J., 1956: On the inclusion of moist adiabatic processes in numerical prediction models. *Ber. d. deutsches Wetterd.*, **5**, No. 38, 82–90.

——, and G. O. Collins, 1955: On the numerical prediction of precipitation. *Mon. Wea. Rev.*, **83**, 53–68.

Smebye, S. J., 1958: Computation of precipitation from large-scale vertical motion. *J. Meteor.*, 547–560.